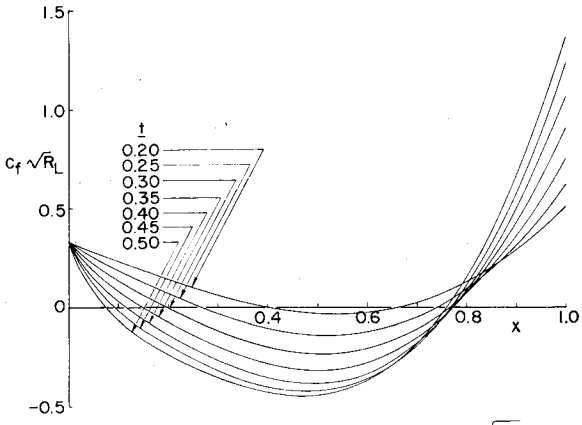

Fig. 1 Variation of local skin-friction coefficient $c_f\sqrt{R_L}$ with x for various values of t. Here $R_L = u_o L/\nu$ with u_o and L denoting a reference velocity and length, respectively.

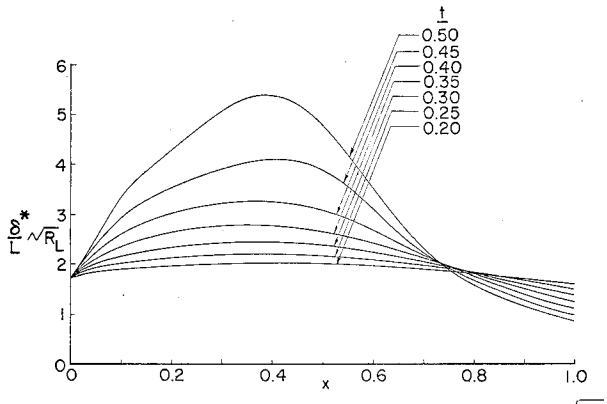

Fig. 2 Variation of dimensions displacement thickness $\delta^*/L\sqrt{R_L}$ with x for various values of t.

is no doubt that were an accurate solution of Eq. (1) computed under conditions of Eq. (2), no singularity would be found either and we believe that those found for the turbulent flows are spurious.

In the third cited example of a singularity,[14] the choice of u_e made the numerical work very difficult, but we maintain that an accurate solution would also be free of singularities for all t. Noting that Walker[15] has also given an example of an unsteady boundary layer with rapid growth of a reversed flow region but no singularity at finite t, we conclude that the answer to the question posed in the introduction is NO!; a singularity cannot develop in Eq. (1) at a finite time if the solution is free from singularities at earlier times.

Acknowledgment

This work was supported by the Office of Naval Research under Contract N00014-77-C-0156.

References

[1] Sears, W.R. and Telionis, D.P., "Boundary-Layer Separation in Unsteady Flow," *SIAM Journal of Applied Mathematics*, Vol. 28, 1975, p. 215.

[2] Riley, N., "Unsteady Laminar Boundary Layers," SIAM Rev., Vol. 17, 1975, p. 274.

[3] Williams, III, J.C. and Johnson, W.D., "Semi-Similar Solutions to Unsteady Boundary-Layer Flows Including Separation," *AIAA Journal*, Vol. 12, 1974, p. 1388.

[4] Brown, S.N., Phil. Trans. Royal Society of London A257, 409, 1965.

[5] Bodonyi, R.J. and Stewartson, K., "The Unsteady Laminar Boundary Layer on a Rotating Disk in a Counter-Rotating Fluid," *Journal of Fluid Mechanics*, Vol. 79, 1977, pp. 669-688.

[6] Carr, L.W., McAlister, K.W., and McCroskey, W.J., "Analysis of the Development of Dynamic Stall Based on Oscillating Airfoil Experiments," NASA TN D-8382, 1977.

[7] Telionis, D.P. and Tsahalis, D.T., "Unsteady Laminar Separation Over Cylinder Started Impulsively From Rest," *Acta Astronautica*, Vol. 1, 1974, p. 1487.

[8] Cebeci, T., "The Laminar Boundary Layer on a Circular Cylinder Started Impulsively From Rest," to appear in *Journal of Computational Physics*, 1978.

[9] Proudman, I. and Johnson, K., "Boundary-Layer Growth Near a Rear Stagnation Point," *Journal of Fluid Mechanics*, Vol. 14, 1962, pp. 161-168.

[10] Patel, V.C. and Nash, J., "Unsteady Turbulent Boundary Layers with Flow Reversal," *Unsteady Aerodynamics*, Kinney, Ed., Vol. 1, 1975, p. 191.

[11] Cebeci, T., Stewartson, K., and Williams, P.G., "On the Response of a Stagnation Boundary Layer to a Change in the External Velocity," to appear in *SIAM Journal of Applied Mathematics*, 1978.

[12] Cebeci, T. and Bradshaw, P. "Momentum Transfer in Boundary Layers," McGraw-Hill/Hemisphere, Washington, D.C., 1977.

[13] Cebeci, T. and Carr, L.W., "A Computer Program for Calculating Laminar and Turbulent Boundary Layers for Two-Dimensional Time-Dependent Flows," NASA TM 78470, March 1978.

[14] Telionis, D.P., Tsahalis, D.T., and Werle, M.J., "Numerical Investigation of Unsteady Boundary-Layer Separation," *Physics of Fluids*, Vol. 16, 1973, p. 968.

[15] Walker, J.D.A., "The Boundary Layer Due to Rectilinear Vortex," Proceedings of Royal Society, A 359, 1978, p. 167.

Reynolds Number Influence on Leeside Flowfields

Joachim Szodruch*
Institut für Luft- und Raumfahrt, Technical University Berlin, Germany

Introduction

LEESIDE flowfields have been of increased interest in the planning and development of supersonic aircraft and hypersonic space shuttle configurations. Although numerous reports have been published, very few systematic investigations are known. In this respect, it seems reasonable to consider first simple shapes like flat delta wings. The results of Refs. 1 and 2 provided a starting point for the author to derive a general description of the different types of flow and their boundaries.[3] In discussing these boundaries it is convenient to use the flow components normal to the leading edge, i.e., α_N and M_N, thus eliminating the sweep angle.

In Fig. 1 the following types of flow have been defined[3]: 1) leading-edge separation, 2) separation with embedded shock, and 3) shock-induced separation. Within the $\alpha_N - M_N$ diagram there exist boundaries, such as the well-known Stanbrook-Squire boundary, over which a continuous change over from one type of flow to the other occurs.

The main variables for the leeside flow over flat and slender delta wings with straight and sharp leading edges are 1) Mach number M_∞, 2) angle of attack α, 3) leading-edge sweep angle Λ, and 4) Reynolds number Re. While account is taken for the first three parameters, the question of Re influence on the flowfield remains to be answered. At hypersonic speeds quite a few investigations on that subject have been carried out (as examples see Refs. 4-6), while on the other hand at supersonic Mach numbers very little is known.[7,8]

Received May 10, 1978; revision received July 5, 1978.

Index category: Supersonic and Hypersonic Flow.

*Research Scientist. Presently at NASA Ames Research Center, Calif.

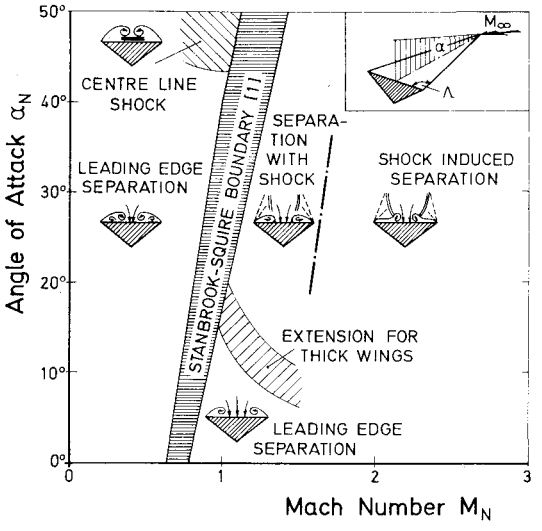

Fig. 1 Flow types and boundaries in $\alpha_N - M_N$ diagram.

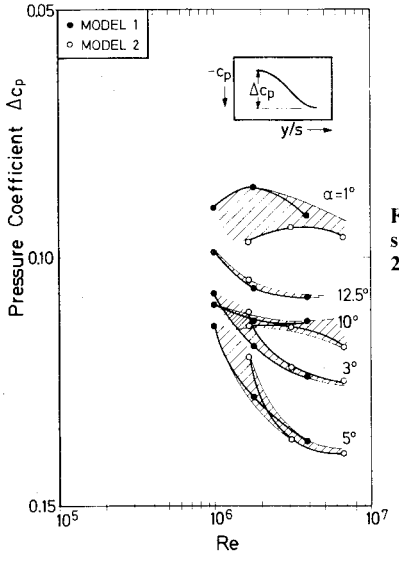

Fig. 2 Influence of *Re* on suction peak level $M_\infty = 2.5$.

This Note discusses some results of *Re* influence on the lee-side flowfield of planar delta wings at supersonic speeds. The freestream conditions have been chosen in a manner that, according to the $\alpha_N - M_N$ diagram in Fig. 1, two types of flow, left and right to the Stanbrook-Squire boundary, can be investigated: leading-edge separation and separation with embedded shock.

Experimental

The experiments were carried out in two wind tunnels [a blowdown-type tunnel at the Cambridge University Engineering Department (CUED), England, and an ejector-type tunnel at the Institut für Luft-und Raumfahrt (ILR), Germany] at Mach numbers of $M_\infty = 2.5$ and 3.5, while the angle of attack varied between $\alpha = 1$ deg and 12.5 deg.

Two delta wing models with different lengths (models 1 and 2 with lengths $\ell = 65$ mm and 111 mm, respectively) were employed having straight, sharp leading edges with a sweep angle $\Lambda = 72.5$ deg. The cross-sectional shape was triangular, giving the models a relative height of $h/\ell = 0.25$. Because of these considerably thick wings, the lower surface shape can not be neglected, however, the results in Fig. 1 were obtained with the same wings and therefore the influence of thickness is not further discussed.

Results and Discussion

On the left side of the Stanbrook-Squire boundary there exists, at $M_\infty = 2.5$, the well-known leading-edge separation.

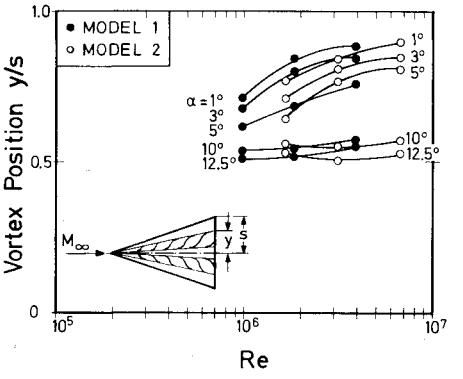

Fig. 3 Influence of *Re* on vortex position $M_\infty = 2.5$.

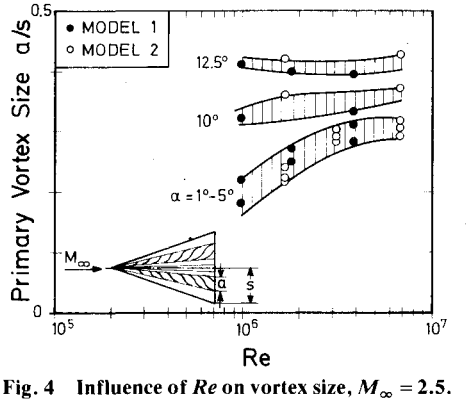

Fig. 4 Influence of *Re* on vortex size, $M_\infty = 2.5$.

Due to varying wind tunnel stagnation pressures and different model lengths, Reynolds numbers between 0.97 and 6.64×10^6 were achieved. In general one expects no influence of *Re* for that kind of flowfield. The separation of the primary vortex is fixed to the leading edge, and only the secondary vortices could be influenced. The latter however do not appear at lower incidences (first appearance just below $\alpha = 10$ deg), since the primary vortex covers the entire field between the leading edge and the attached flow near the centerline. On the other hand, it can be assumed that at higher angles of attack the flow on the lee side is already turbulent. All together, no major alternation of this type of flow seems to occur with changes in *Re*.

Pressure measurements and different methods of flow visualization confirm the foregoing considerations. Static pressures over the span show the typical suction peak near the leading edge. The higher pressures of the attached flow near the centerline vary only slightly, and, on the assumption that this flow regime is not influenced by *Re* effects, it is reasonable to plot the pressure difference Δc_p between the maximum and minimum level to account for possible effects on the vortex. The result is shown in Fig. 2. At low incidences (except for $\alpha = 1$ deg), the suction peak is increasing with *Re* indicating a rise of vortex intensity. At higher incidences, i.e., $\alpha = 10$ deg and 12.5 deg, the suction peak is almost at the same level, except for the smaller Reynolds number where a slight increase is recognized.

Since the pressure level underneath the primary vortex decreases as much as 15% with increasing *Re*, this might lead to the conclusion that the dimensions of the flowfield alter as well. One reliable method of detecting the vortex center is given by oil film pictures. In Ref. 3 it has been shown that the vortex center lies above the line that is formed by the outboard moving oil streaks of the typical "feather" pattern. The evaluation of the oil film pattern is plotted in Fig. 3. For angles of attack up to $\alpha = 5$ deg the vortex center moves outboard with increasing *Re*, but does not change position at high incidences. Here it is still uncertain if just the vortex

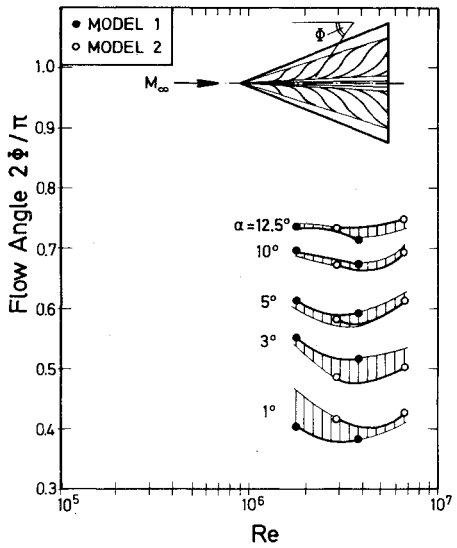

Fig. 5 Influence of *Re* on outflow angle of oil streaks, $M_\infty = 2.5$.

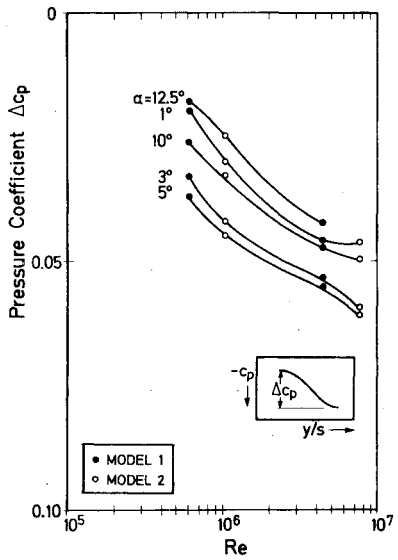

Fig. 6 Influence of *Re* on suction peak level, $M_\infty = 3.5$.

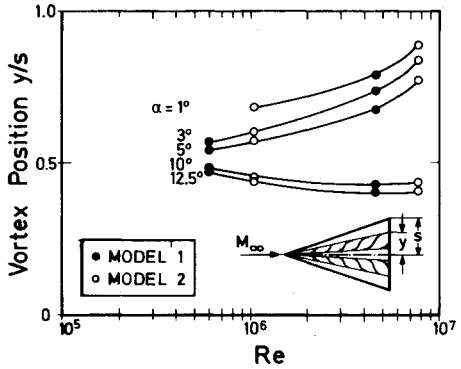

Fig. 7 Influence of *Re* on vortex position, $M_\infty = 3.5$.

shifts towards the leading edge, which would imply the growing of the area of attached flow near the centerline. The answer is given by Fig. 4, where the vortex size is plotted vs *Re*. Here it becomes evident that the vortex grows in size at the same rate at which the vortex center moves outboard. In this way it is confirmed that no effects of *Re* exist on the attached flow in the middle of the wing.

The pressure results indicate different vortex intensities as *Re* is changed. In a first attempt one can determine the intensity from oil flow experiments, using the outflow angle of oil streaks underneath the vortex as an indicator. Thus, in Fig. 5 the flow angle does not vary with *Re* at fixed angles of attack, however, one has to consider the increasing vortex size. It is believed that the effects of higher intensities and growing vortex size on the outflow angle just cancel each other. This implies the increasing vortex intensity with higher *Re*.

In summary, it has been shown that, in general, the flow type of leading-edge separation remains unchanged with an increase in Reynolds number. Only variations in vortex center position, vortex size, and suction peak pressure were obtained for low incidences. At higher angles of attack the turbulent flow and the strong primary vortex dominate the flowfield, thus leaving no possibilities for *Re* effects, even on the secondary vortex.

On the right-hand side of the Stanbrook-Squire boundary there exist at $M_\infty = 3.5$ two types of flow depending on the angle of attack. Because of the considerably high thickness ratio, leading-edge separation still occurs for low angles of attack, while values of $\alpha > 5$ deg lead to a flow type called separation with embedded shock. The latter describes a flowfield with detached flow at the leading edge, very similar to the separation bubbles over airfoils. Despite the fact that the bow shock is detached from the leading edge, the crossflow velocity component is supersonic. Therefore, expansion waves are present above the separation bubble and embedded shocks are formed further inboard. Thus, the term separation with shock accounts for the fact that separation and embedded shock appear independently but not without influence on each other. From a detailed knowledge of the flowfield one expects no major *Re* effect on leading-edge separation (see results for $M_\infty = 2.5$). On the other hand, two-dimensional flows have shown sensitivity of separation bubbles to *Re* changes. We can therefore expect that the expansion and embedded shock might also be affected. The following results for *Re* variation between 0.6 and 7.57×10^6 at $M_\infty = 3.5$ exhibit the influence on the different flow types.

The attached flow near the centerline is still regarded as independent of *Re* and again the difference between maximum and minimum pressure is plotted in Fig. 6. For leading-edge separation, i.e., at low incidences, the suction peak induced by the vortex is increasing with higher *Re* as already seen for $M_\infty = 2.5$. At higher angles of attack ($\alpha = 10$ deg and 12.5 deg) the pressure coefficient Δc_p is still rising with *Re*. This development is due to a different effect, with the low pressure near the leading edge being induced by an expansion instead of vortices. Since the expansion takes place above the separation bubble, which decreases in height with rising *Re*, the effective expansion angle increases. This leads to the same behavior of the pressure Δc_p vs *Re* as in the case of leading-edge separation. The geometric variations of the flowfield are shown in Figs. 7 and 8. For low angles of attack, i.e., leading-edge separation, the vortex center moves outboard as expected from the foregoing results. The vortex also grows in size, with the area of attached flow near the centerline remaining roughly constant. At higher incidences the vortex center shows an almost fixed spanwise position, with a small tendency to move inboard with higher *Re*. The vortex size is nearly constant as well, although it seems to grow just slightly. From Schlieren observations it is concluded that the separation bubble decreases considerably in height with little effect in the spanwise direction. The influence on vortex intensity is not further discussed here, since no distinct results could be obtained. It should be noted however, that within the separation bubble a vortex-like flow exists, because of the pressure gradient between the centerline and leading-edge region. As the Reynolds number increases, the pressure difference rises, leading to the assumption of increasing vortex intensity.

Although *Re* variation within the tested limits does not alter the types of flow, a considerable shifting of vortex

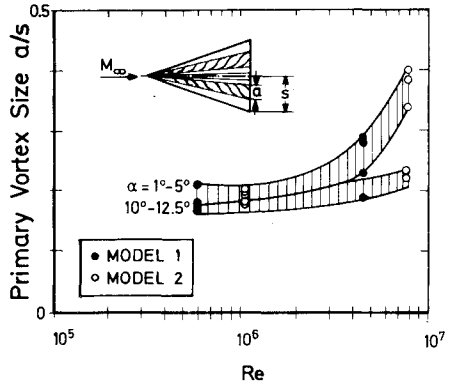

Fig. 8 Influence of *Re* on vortex size, $M_\infty = 3.5$.

position and pressure level has been observed. This is certainly true for the flow type with leading-edge separation and agrees in general with results of Ref. 8. However, for the type of flow described as separation with shock, further considerations are worthwhile. The experiments seem to show that the separation bubble flattens for higher Reynolds numbers, moving closer to the upper surface until the flow near the leading edge is attached. Thus another type of flow, the well-known shock-induced separation, is established. According to the $\alpha_N - M_N$ diagram of Fig. 1 and the preceding conclusions, shock-induced separation is obtained at either higher Mach numbers or higher Reynolds numbers. The $\alpha_N - M_N$ diagram is therefore strictly valid only for fixed Reynolds numbers, a fact which is also confirmed by results at hypersonic Mach numbers.

Conclusion

The influence of Reynolds number on the types of flow left and right to the Stanbrook-Squire boundary has been examined. For leading-edge separation conditions, the vortex position and intensity, and thus the suction pressure, vary while the type of flow remains nearly unchanged. In the region of separation with embedded shock, *Re* affects not only the shape of the separation bubble and pressure level near the leading edge but the type of flow as well. At sufficiently high Reynolds numbers the flow type of separation with shock changes to one with shock-induced separation. In agreement with hypersonic investigations it turns out that the flow regimes sketched in the $\alpha_N - M_N$ diagram are effective only for fixed *Re*.

References

[1] Stanbrook, A. and Squire, L.C., "Possible Types of Flow at Swept Leading Edges," *Aeronautical Quarterly*, Vol. 15, 1960, pp. 72-82.

[2] Squire, L.C., "Flow Regimes Over Delta Wings at Supersonic and Hypersonic Speeds," *Aeronautical Quarterly*, Vol. 27, 1976, pp. 1-14.

[3] Szodruch, J., "Leeseiten-Strömung schlanker Deltaflügel endlicher Dicke," ILR-Bericht Nr. 23, Technical University, Berlin, 1977.

[4] Hefner, J.N., "Lee Surface Heating and Flow Phenomena on Space Shuttle Orbiters at Large Angles of Attack and Hypersonic Speeds," NASA TND-7088, 1972.

[5] Rao, D.M. and Whitehead, A.H., "Lee Side Vortices on Delta Wings at Hypersonic Speeds," *AIAA Journal*, Vol. 10, Nov. 1972, pp. 1458-1465.

[6] Dunavant, J.C., Narayan, K.Y., and Walberg, G.D., "A Survey of Leeside Flow and Heat Transfer on Delta Planform Configurations," AIAA Paper 76-118, 1976.

[7] Thomann, H., "Measurement of Heat Transfer, Recovery Temperature and Pressure Distribution on Delta Wings at M = 3," FFA Report 93, Sweden, 1962.

[8] Lee, G.H., "Note on the Flow Around Delta Wings with Sharp Leading Edges," A.R.C., R&M No. 3070, 1955.

Real Gas Effects in a Pulsed Laser Propulsion System

Sharad Chandra Purohit*
Vikram Sarabhai Space Centre, Trivandrum, India

RECENTLY, Simons and Pirri[1] developed a fluid mechanical model for a pulsed laser propulsion system and showed that it is an efficient steady-state system. One of the assumptions made by them is that the gas is ideal. The purpose of this Note is to study the change in the functional values of energy efficiency and specific impulse when the gas is almost ideal.

The modified equation of state in a simplified form, as given by Landau and Lifshitz,[2] is

$$p = \rho RT(1 + b\rho) \tag{1}$$

where b is the molecular weight. Using notation similar to that of Simons and Pirri, the basic transformed equations can be written as

$$\frac{dg}{d\eta} - \frac{hf}{2\beta} + \frac{f}{\beta}[(1-\beta)h - \eta]\frac{dh}{d\eta} = 0 \tag{2}$$

$$\frac{dh}{d\eta} - \frac{2}{(1-\beta)} - \frac{\eta}{(1-\beta)}\frac{1}{f}\frac{df}{d\eta} + \frac{h}{f}\frac{df}{d\eta} + 2\frac{h}{\eta} = 0 \tag{3}$$

$$[(1-\beta)h - \eta]\frac{dg}{d\eta} - g\frac{df}{d\eta}[(1-\beta)h - \eta]\left[\frac{\alpha}{\beta} + \frac{\gamma}{f} + \frac{\alpha}{\beta(\gamma-1)}\left(1 + \frac{\alpha}{\beta(\gamma-1)}f\right)^{-1}\right] + g\left[2\gamma - 3 + 2f\frac{\alpha}{\beta} + 2f\frac{\alpha}{\beta(\gamma-1)}\left(1 + \frac{\alpha}{\beta(\gamma-1)}f\right)^{-1}\right] = 0 \tag{4}$$

While strong shock conditions are defined as (see Rao and Purohit[3]):

$$\rho_s(t) = \rho_\ell(t)/\beta$$

$$p_s(t) = (1-\beta)\rho_\ell(t)V_s^2(t)$$

$$u_s(t) = (1-\beta)\ V_s(t) \tag{5}$$

where

$$\beta = \frac{(\gamma - 1 - \alpha) + \sqrt{(\gamma-1-\alpha)^2 + 4\alpha(\gamma+1)}}{2(\gamma+1)}$$

$$\alpha = b\ \rho_\ell(t)\ (\gamma - 1)$$

α is a nonideal gas parameter and $\alpha = 0$ is a particular case discussed by Simons and Pirri. β is a monotonically increasing function of positive α.

By using a fourth-order Runge-Kutta procedure, the basic equations (2-4) are solved from $\eta = 1$ to $\eta = 0$ together with the

Received June 15, 1978; revision received Aug. 10, 1978.

Index categories: Nozzle and Channel Flow; Shock Waves and Detonations.

*Scientist, Applied Mathematics Section.